Mechanics of Advanced Materials and Structures, 17:393–405, 2010

ISSN: 1537-6494 print / 1537-6532 online
DOI: 10.1080/15376494.2010.483321

Taylor & Francis
Taylor & Francis Group

An Analytical Approach for an Adhesive Layer in a Graded Elastic Wedge

Efstathios E. Theotokoglou,[1] Ioannis H. Stampouloglou,[1] and Glaucio H. Paulino[2]

[1]*School of Applied Mathematical and Physical Sciences, Department of Mechanics-Laboratory of Strength of Materials, The National Technical University of Athens, Athens, Greece*

[2]*Department of Civil and Environmental Engineering, University of Illnois at Urbana—Champaign, Champaign, Illinois, United States*

In this paper the influence of an adhesive layer in a graded elastic wedge consisted of two subwedges radially bonded, is investigated by means of linear elasticity. The adhesive layer in the analytical solution is simulated either by an interface or by an infinitesimal subwedge of very small wedge-angle. The graded character of the wedges is given either by a linearly varying or by an exponentially varying shear modulus. The inhomogeneous anisotropic self-similar bi-wedge and tri-wedge, loaded by a concentrated force at their apex, are studied analytically under plane strain or generalized plane stress conditions, using the self-similarity property. Based on the separation of loading in each subwedge and on the continuity of displacements at the interface, an analytic solution is deduced for the stress and displacements fields. Applications have been made in the case of a graded bi-wedge and a composite tri-wedge, in which for specific values of gradation, the stress and displacements fields are determined.

Keywords functionally graded materials, angularly inhomogeneous wedge, self-similarity property, plane elasticity problem, adhesive layer, multi-material junction

1. INTRODUCTION

A very interesting problem in anisotropic and inhomogeneous elastic materials [1–25] is that of cylinders subjected in pure torsion and possessing cylindrical orthotropy with a variation of the materials properties [2]. In another interesting problem, Chung and Ting [8] and Ting [10] gave the solution of an anisotropic half-space with elastic moduli depending upon one coordinate, the angle, θ, when the loads on the half-space are represented by a straight line of force. Finally Carpinteri, and Paggi [22] studied the order of singularity of multi-material junctions where the Young's modulus varied only with the angle, θ. These kinds of problems are called "angularly inhomogeneous problems."

The anisotropic wedge problem has already been confronted by many researchers [10, 12, 15, 17–22, 24]. In these investigations, the wedge problem is studied under a generally applied loading at the faces and/or the apex of the wedge. The linear elastostatic problem of a generally anisotropic and angularly inhomogeneous plane wedge loaded by a concentrated force at its apex is studied in Stampouloglou and Theotokoglou [20].

A graded wedge (angularly inhomogeneous) may represent a multi-wedge with a lot of equiangular subwedges of different material. On the other hand the increasing use of adhesive joints in many practical applications requires the understating of the stress distributions in these joints [26]. Two different graded wedges may be glued together by an adhesive layer. This type of connection is important from the engineering point of view because it may appear in brazed tri-material systems, in the region of ply drop in composites, and at the edge close-out of sandwich beams.

The purpose of our paper is to study, by means of elasticity, a plane graded bi-wedge and to investigate the influence of an adhesive bonding layer between the two graded sub-wedges. In order to keep the self-similarity property in the proposed analytical solution, the adhesive layer is simulated either by an interface (a subwedge of zero wedge-angle) or by an infinitesimal subwedge of very small wedge-angle with elastic constants those of an isotropic adhesive material. In the first case an analytical solution is obtained for a graded bi-wedge whereas in the second case an analytical solution for a tri-wedge results.

The multi-material wedge with a lot of equiangular subwedges of different material, which may appear in half spaces with an "angularly inhomogeneous" variation of the elastic moduli [6], is represented in this study by a graded wedge. The graded character of the wedge is approximated by:

(i) a linearly varying shear modulus and a constant Poisson's ratio for each subwedge

Received 11 August 2008; accepted 15 June 2009.

Address correspondence to Efstathios E. Theotokoglou, School of Applied Mathematical and Physical Sciences, Department of Mechanics-Laboratory of Strength of Materials, The National Technical University of Athens, Zografou Campus, Theocaris Blvd., Gr-0157 73, Athens, Greece. E-mail: stathis@central.ntua.gr

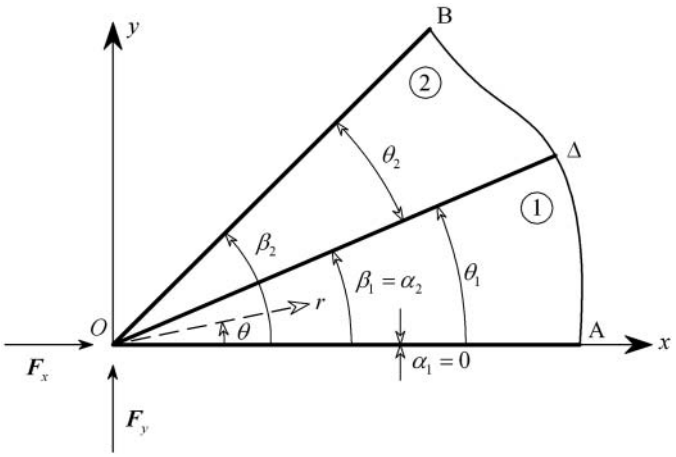

FIG. 1. A graded bi-wedge under a concentrated load at its apex.

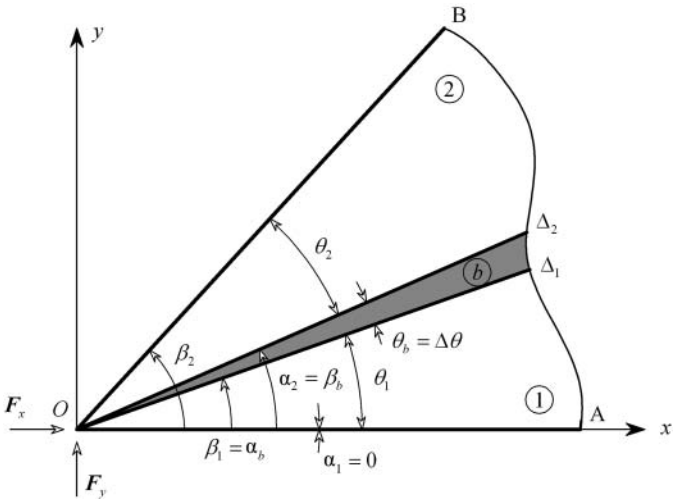

FIG. 2. A composite wedge consisting of two graded subwedges and an infinitesimal third subwedge under a concentrated load at is apex.

(ii) an exponentially varying shear modulus and a constant Poisson's ratio for each subwedge.

These types of approximations are the most popular approaches for considering elastic nonhomogeneity [4, 6, 25].

Let us consider a graded linear elastic wedge of angle $\theta_w(=\theta_1+\theta_2)$, loaded by a concentrated force at is apex. It is also supposed that the wedge consisting of two subwedges, is radially bonded (Figure 1). In each subwedge $j(=1,\ 2)$, the angularly varying shear modulus G, equal to the Lamé [5] constant $\mu(\mu = G)$, is given by:

(i) a linear variation

$$\mu^{(j)}(\theta) = \mu_j + \xi_j\theta, \quad \alpha_j \le \theta \le \beta_j; \quad j = 1, 2 \tag{1}$$

where $\mu_j, \xi_j (j = 1,\ 2)$ known constants.

(ii) an exponential variation

$$\mu^{(j)}(\theta) = \mu_{o_j} e^{d_j(\theta - \frac{\alpha_j+\beta_j}{2})}, \quad \alpha_j \le \theta \le \beta_j,$$
$$\theta_j = \beta_j - \alpha_j; \quad j = 1, 2 \tag{2}$$
$$\mu_{o_j} = \mu^{(j)}\left(\theta = \frac{\alpha_j+\beta_j}{2}\right); \quad j = 1, 2 \tag{3}$$
$$d_j = -\frac{2}{\theta_j}\ln\left(1 - \zeta_j\frac{\theta_j}{2}\right), \quad \theta_j = \beta_j - \alpha_j,$$
$$\zeta_j = \xi_j/\mu_{o_j}; \quad j = 1, 2 \tag{4}$$

where ξ_j $(j = 1, 2)$ is a known constant.

On the other hand a composite wedge $(\theta_w = \theta_1 + \theta_b + \theta_2)$ is considered consisting of two graded subwedges $(j = 1, 2)$ and an infinitesimal third subwedge of angle $\theta_b = \Delta\theta$ (Figure 2). In each subwedge the angularly varying shear modulus is given by:

(i) a linear variation

$$\mu^{(1)}(\theta) = \mu_1 + \xi_1\theta, \beta_1 - \alpha_1 = \theta_1,$$
$$\alpha_1(=0) \le \theta \le \beta_1\,(=\theta_1)$$
$$\mu = \mu_b, \xi_b = 0, \beta_b - \alpha_b = \theta_b = \Delta\theta,$$
$$\alpha_b\,(=\theta_1) \le \theta \le \beta_b\,(=\theta_1+\Delta\theta)$$
$$\mu^{(2)}(\theta) = \mu_2 + \xi_2\theta, \beta_2 - \alpha_2 = \theta_2, \alpha_2\,(=\theta_1+\Delta\theta)$$
$$\le \theta \le \beta_2\,(=\theta_1+\theta_2+\Delta\theta) \tag{5}$$

where $\mu_j, \xi_j (j = 1, b, 2)$ known constants.

(ii) an exponential variation

$$\mu^{(1)}(\theta) = \mu_{o_1} e^{d_1(\theta-\theta_1/2)}, \theta_1 = \beta_1 - \alpha_1,$$
$$\alpha_1\,(=0) \le \theta \le \beta_1\,(=\theta_1)$$
$$\mu^{(b)}(\theta) = \mu_b, \theta_b = \beta_b - \alpha_b = \Delta\theta,$$
$$\alpha_b\,(=\theta_1) \le \theta \le \beta_b\,(=\theta_1+\theta_b)$$
$$\mu^{(2)}(\theta) = \mu_{o_2} e^{d_2(\theta-\theta_1-\theta_b-\theta_2/2)}, \theta_2 = \beta_2 - \alpha_2,$$
$$\alpha_2\,(=\theta_1+\theta_b) \le \theta \le \beta_2\,(=\theta_1+\theta_2+\theta_b) \tag{6}$$

where $\mu_{o_j}, d_j (j = 1, 2)$ are given by relations (3) and (4) and μ_b known constant.

Based on the self-similarity property [5, 20, 21] and the graded character of an angularly inhomogeneous wedge, the stress and displacement fields have been determined for each case of gradation. Finally applications have been made for a graded bi-wedge of angle $\theta_w = \pi/2$ and a composite tri-wedge of angle $\theta_w \cong \pi/2$, in which for specific values of gradation, the stress and displacements fields have been determined. The stress fields in the case of the composite tri-wedge $(\theta_w \cong \pi/2)$ are compared with the results obtained by the finite element analysis.

2. THE INHOMOGENEOUS ANISOTROPIC SELF-SIMILAR BI-WEDGE LOADED BY A CONCENTRATED FORCE AT ITS APEX

Let an infinite plane angularly inhomogeneous bi-wedge with a concentrated force at its apex (Figure 1),

$$\begin{aligned} \boldsymbol{F} &= \boldsymbol{F}_x + \boldsymbol{F}_y = \boldsymbol{F}_1 + \boldsymbol{F}_2 \\ \boldsymbol{F}_j &= \boldsymbol{F}_{j_x}\boldsymbol{e}_x + \boldsymbol{F}_{j_y}\boldsymbol{e}_y;\ j = 1,2 \end{aligned} \tag{7}$$

where $F_j(F_{j_x}, F_{j_y})$ the concentrated force acting on the subwedge $j(=1,2)$.

Taking into consideration the self-similarity property [5, 20] and the graded character of an angularly inhomogeneous wedge, the radial stress field of each subwedge ($\sigma_{r\theta}^{(j)} = \sigma_{\theta\theta}^{(j)} = 0$, $j = 1, 2$) [5, 20], in the polar coordinate system (r, θ)(Figure 1), is given by:

$$\begin{aligned} \sigma_{rr}^{(j)}(r,\theta) &= \frac{8\mu^{(j)}(\theta)}{r(\kappa_j+1)}(\Gamma_j\cos\theta + \Delta_j\sin\theta), \\ &\alpha_j \le \theta \le \beta_j;\ \ j = 1,2\,, \end{aligned} \tag{8}$$

whereas the displacements field $\boldsymbol{u}^{(j)}(\boldsymbol{u}_r^{(j)}, \boldsymbol{u}_\theta^{(j)})$ of each subwedge $j(=1,2)$ using Michell's Tables [5, 20, 24], is written as:

$$\begin{aligned} u_r^{(j)} &= (\Gamma_j\cos\theta + \Delta_j\sin\theta)\ln r \\ &\quad + \theta\frac{\kappa_j-1}{\kappa_j+1}(\Gamma_j\sin\theta - \Delta_j\cos\theta);\ j = 1,2 \\ u_\theta^{(j)} &= -\left(\frac{2}{\kappa_j+1} + \ln r\right)(\Gamma_j\sin\theta - \Delta_j\cos\theta) \\ &\quad + \theta\frac{\kappa_j-1}{\kappa_j+1}(\Gamma_j\cos\theta + \Delta_j\sin\theta);\ j = 1,2 \end{aligned} \tag{9a}$$

Taking from relations (9a) the difference of displacements fields, $\boldsymbol{u}^{(j)}(r,\theta) - \boldsymbol{u}^{(j)}$ $(r = 1, \theta)$, it is obtained a displacements field, $\bar{u}^{(j)}(\bar{u}_r^{(j)}, \bar{u}_\theta^{(j)})$, free from rigid body displacements, given by [20, 24]:

$$\bar{\boldsymbol{u}}^{(j)}(r,\theta) = \boldsymbol{u}^{(j)}(r,\theta) - \boldsymbol{u}^{(j)}(r=1,\theta);\ j = 1,2,$$

or

$$\begin{aligned} \bar{u}_r^{(j)}(r,\theta) &= (\Gamma_j\cos\theta + \Delta_j\sin\theta)\ln r, \quad \bar{u}_\theta^{(j)}(r,\theta) \\ &= (-\Gamma_j\sin\theta + \Delta_j\cos\theta)\ln r, \quad \alpha_j \le \theta \le \beta_j;\ \ j = 1,2, \end{aligned} \tag{9b}$$

where $\kappa_j = 3-4\nu_j$ for plane strain and $\kappa_j = (3-\nu_j)/(1+\nu_j)$ for generalized plane stress conditions, Poisson's ratio, and

$$\begin{aligned} \Gamma_j &= -\frac{F_{j_x}[\Psi_j(\beta_j) - \Psi_j(\alpha_j) + P_j(\alpha_j) - P_j(\beta_j)] - F_{j_y}[Q_j(\beta_j) - Q_j(\alpha_j)]}{[P_j(\beta_j) - P_j(\alpha_j)][\Psi_j(\beta_j) - \Psi_j(\alpha_j) + P_j(\alpha_j) - P_j(\beta_j)] - [Q_j(\beta_j) - Q_j(\alpha_j)]^2} \\ \Delta_j &= \frac{F_{j_x}[Q_j(\beta_j) - Q_j(\alpha_j)] - F_{j_y}[P_j(\beta_j) - P_j(\alpha_j)]}{[P_j(\beta_j) - P_j(\alpha_j)][\Psi_j(\beta_j) - \Psi_j(\alpha_j) + P_j(\alpha_l) - P_j(\beta_j)] - [Q_j(\beta_j) - Q_j(\alpha_j)]^2} \end{aligned} \tag{10}$$

with

$$\begin{aligned} P_j(\theta) &= \frac{8}{\kappa_j+1}\int \mu^{(j)}(\theta)\cos^2\theta d\theta, \\ Q_j(\theta) &= \frac{8}{\kappa_j+1}\int \mu^{(j)}(\theta)\cos\theta\sin\theta d\theta, \\ \Psi_j(\theta) &= \frac{8}{\kappa_j+1}\int \mu^{(j)}(\theta)d\theta; \quad j = 1,2 \end{aligned} \tag{11}$$

For the case of a linearly varying shear modulus $\mu^{(j)}(j = 1, 2)$, from relations (10) and (11) and taking into consideration relations (1), it is obtained:

$$\begin{aligned} \Gamma_j &= -\gamma_j F_{j_x} + \eta_j F_{j_y};\ \ j = 1,2 \\ \Delta_j &= \eta_j F_{j_x} - \delta_j F_{j_y};\ \ j = 1,2 \end{aligned} \tag{12}$$

where

$$\begin{aligned} \gamma_j &= (\kappa_j+1)\frac{4\left(\mu_j + \xi_j\frac{\theta_j+2\alpha_j}{2}\right)[\theta_j - \sin\theta_j\cos(\theta_j+2\alpha_j)] - 2\xi_j\sin(\theta_j+2\alpha_j)(\theta_j\cos\theta_j - \sin\theta_j)}{16\left(\mu_j + \xi_j\frac{\theta_j+2\alpha_j}{2}\right)^2(\theta_j^2 - \sin^2\theta_j) - 4\xi_j^2(\theta_j\cos\theta_j - \sin\theta_j)^2} \\ \delta_j &= (\kappa_j+1)\frac{4\left(\mu_j + \xi_j\frac{\theta_j+2\alpha_j}{2}\right)[\theta_j + \sin\theta_j\cos(\theta_j+2\alpha_j)] + 2\xi_j\sin(\theta_j+2\alpha_j)(\theta_j\cos\theta_j - \sin\theta_j)}{16\left(\mu_j + \xi_j\frac{\theta_j+2\alpha_j}{2}\right)^2(\theta_j^2 - \sin^2\theta_j) - 4\xi_j^2(\theta_j\cos\theta_j - \sin\theta_j)^2} \\ \eta_j &= (\kappa_j+1)\frac{4\left(\mu_j + \xi_j\frac{\theta_j+2\alpha_j}{2}\right)\sin\theta_j\sin(\theta_j+2\alpha_j) - 2\xi_j\cos(\theta_j+2\alpha_j)(\theta_j\cos\theta_j - \sin\theta_j)}{16\left(\mu_j + \xi_j\frac{\theta_j+2\alpha_j}{2}\right)^2(\theta_j^2 - \sin^2\theta_j) - 4\xi_j^2(\theta_j\cos\theta_j - \sin\theta_j)^2} \end{aligned} \tag{13}$$

Taking into consideration the boundary conditions along the interface (OΔ) (Figure 1),

$$\begin{aligned}\bar{u}_r^{(1)}(r,\theta=\beta_1)&=\bar{u}_r^{(2)}(r,\theta=\beta_1),\\ \bar{u}_\theta^{(1)}(r,\theta=\beta_1)&=\bar{u}_\theta^{(2)}(r,\theta=\beta_1),\end{aligned}\tag{14}$$

and the separation of the force in each subwedge (relation (7)), it is finally obtained

$$\begin{aligned}\Gamma_1\cos\beta_1+\Delta_1\sin\beta_1&=\Gamma_2\cos\beta_1+\Delta_2\sin\beta_1\\ \Gamma_1\sin\beta_1-\Delta_1\cos\beta_1&=\Gamma_2\sin\beta_1-\Delta_2\cos\beta_1\\ F_{1_x}+F_{2_x}&=F_x\\ F_{1_y}+F_{2_y}&=F_y\end{aligned}\tag{15}$$

From the solution of the system (15), we have

$$\begin{aligned}F_{1_x}&=\frac{[-\eta_2(\eta_1+\eta_2)+\gamma_2(\delta_1+\delta_2)]F_x+(-\delta_1\eta_2+\delta_2\eta_1)F_y}{-(\eta_1+\eta_2)^2+(\gamma_1+\gamma_2)(\delta_1+\delta_2)}\\ F_{1_y}&=\frac{(\gamma_2\eta_1-\gamma_1\eta_2)F_x+[-\eta_2(\eta_1+\eta_2)+\delta_2(\gamma_1+\gamma_2)]F_y}{-(\eta_1+\eta_2)^2+(\gamma_1+\gamma_2)(\delta_1+\delta_2)}\\ F_{2_x}&=\frac{[-\eta_1(\eta_1+\eta_2)+\gamma_1(\delta_1+\delta_2)]F_x+(-\delta_2\eta_1+\delta_1\eta_2)F_y}{-(\eta_1+\eta_2)^2+(\gamma_1+\gamma_2)(\delta_1+\delta_2)}\\ F_{2_y}&=\frac{(\gamma_1\eta_2-\gamma_2\eta_1)F_x+[-\eta_1(\eta_1+\eta_2)+\delta_1(\gamma_1+\gamma_2)]F_y}{-(\eta_1+\eta_2)^2+(\gamma_1+\gamma_2)(\delta_1+\delta_2)}\end{aligned}\tag{16a}$$

provided that

$$-(\eta_1+\eta_2)^2+(\gamma_1+\gamma_2)(\delta_1+\delta_2)\neq 0$$

From relations (12) and (16a), it is obtained

$$\begin{aligned}\Gamma_1&=-\gamma_1F_{1_x}+\eta_1F_{1_y}=\frac{\left[\gamma_1\eta_2^2+\gamma_2\eta_1^2-\gamma_1\gamma_2(\delta_1+\delta_2)\right]F_x+[\gamma_1\delta_1\eta_2+\gamma_2\delta_2\eta_1-\eta_1\eta_2(\eta_1+\eta_2)]F_y}{-(\eta_1+\eta_2)^2+(\gamma_1+\gamma_2)(\delta_1+\delta_2)}\\ \Gamma_2&=-\gamma_2F_{2_x}+\eta_2F_{2_y}=\Gamma_1\\ \Delta_1&=\eta_1F_{1_x}-\delta_1F_{1_y}=\frac{[\gamma_1\delta_1\eta_2+\gamma_2\delta_2\eta_1-\eta_1\eta_2(\eta_1+\eta_2)]F_x+\left[\delta_1\eta_2^2+\delta_2\eta_1^2-\delta_1\delta_2(\gamma_1+\gamma_2)\right]F_y}{-(\eta_1+\eta_2)^2+(\gamma_1+\gamma_2)(\delta_1+\delta_2)}\\ \Delta_2&=\eta_2F_{2_x}-\delta_2F_{2_y}=\Delta_1\end{aligned}\tag{16b}$$

On the other hand, in the case of an exponentially varying shear modulus, from relations (10), (11), (2), and (3), the coefficients γ_j, η_j and δ_j $(j=1,2)$ of relations (12), are given by:

$$\begin{aligned}\gamma_j&=\frac{d_j^2(\kappa_j+1)}{8\mu_{o_j}}\left\{\frac{\left(\frac{d_j^2+4}{2d_j}-\sin 2\beta_j-\frac{d_j}{2}\cos 2\beta_j\right)e^{\frac{1}{2}d_j\theta_j}-\left(\frac{d_j^2+4}{2d_j}-\sin 2\alpha_j-\frac{d_j}{2}\cos 2\alpha_j\right)e^{-\frac{1}{2}d_j\theta_j}}{e^{d_j\theta_j}+e^{-d_j\theta_j}-\left(2+d_j^2\sin^2\theta_j\right)}\right\}\\ \delta_j&=\frac{d_j^2(\kappa_j+1)}{8\mu_{o_j}}\left\{\frac{\left(\frac{d_j^2+4}{2d_j}+\sin 2\beta_j+\frac{d_j}{2}\cos 2\beta_j\right)e^{\frac{1}{2}d_j\theta_j}-\left(\frac{d_j^2+4}{2d_j}+\sin 2\alpha_j+\frac{d_j}{2}\cos 2\alpha_j\right)e^{-\frac{1}{2}d_j\theta_j}}{e^{d_j\theta_j}+e^{-d_j\theta_j}-\left(2+d_j^2\sin^2\theta_j\right)}\right\}\\ \eta_j&=\frac{d_j^2(\kappa_j+1)}{8\mu_{o_j}}\left\{\frac{\left(\frac{d_j}{2}\sin 2\beta_j-\cos 2\beta_j\right)e^{\frac{1}{2}d_j\theta_j}-\left(\frac{d_j}{2}\sin 2\alpha_j-\cos 2\alpha_j\right)e^{-\frac{1}{2}d_j\theta_j}}{e^{d_j\theta_j}+e^{-d_j\theta_j}-\left(2+d_j^2\sin^2\theta_j\right)}\right\}\end{aligned}\tag{17}$$

Relations (16) are valid either in the case of linearly varying shear modulus or in the case of exponentially varying shear modulus, where the γ_j, δ_j and η_j coefficients are taken either from relations (13) or from relations (17).

3. AN INFINITESIMAL ISOTROPIC ADHESIVE LAYER BONDED BETWEEN TWO GRADED SUBWEDGES

Let an infinitesimal adhesive layer bonded between two graded subwedges (Figure 2). The problem is reduced to the study of a tri-wedge loaded by a concentrated force at its apex.

Let ε the average thickness of the infinitesimal adhesive layer and R_o the maximum radius of the considered sector. The angle θ_b of the subwedge (b) which simulates the infinitesimal

adhesive layer is defined as:

$$\theta_b = \Delta\theta = \frac{2\varepsilon}{R_o} \tag{18}$$

Because of the infinitesimal angle $\theta_b\,(=\Delta\theta)$, an order of approximation $O(\Delta\theta^2)$ is supposed, namely:

$$\begin{aligned}&\sin\Delta\theta \cong \Delta\theta,\ \cos\Delta\theta \cong 1,\ \sin(\varphi+\Delta\theta) \cong \sin\varphi + \Delta\theta\cos\varphi,\\ &\cos(\varphi+\Delta\theta) \cong \cos\varphi - \Delta\theta\sin\varphi\end{aligned} \tag{19}$$

Taking into consideration relations (5), (19), and (13) ($j = 1, b, 2$) in the case of a linearly varying shear modulus, we have:

$$\begin{aligned}
\gamma_1 &= (\kappa_1+1)\frac{4\left(\mu_1+\xi_1\frac{\theta_1}{2}\right)(\theta_1-\sin\theta_1\cos\theta_1) - 2\xi_1\sin\theta_1(\theta_1\cos\theta_1-\sin\theta_1)}{16\left(\mu_1+\xi_1\frac{\theta_1}{2}\right)^2\left(\theta_1^2-\sin^2\theta_1\right) - 4\xi_1^2(\theta_1\cos\theta_1-\sin\theta_1)^2}\\
\delta_1 &= (\kappa_1+1)\frac{4\left(\mu_1+\xi_1\frac{\theta_1}{2}\right)(\theta_1+\sin\theta_1\cos\theta_1) + 2\xi_1\sin\theta_1(\theta_1\cos\theta_1-\sin\theta_1)}{16\left(\mu_1+\xi_1\frac{\theta_1}{2}\right)^2\left(\theta_1^2-\sin^2\theta_1\right) - 4\xi_1^2(\theta_1\cos\theta_1-\sin\theta_1)^2},\\
\eta_1 &= (\kappa_1+1)\frac{4\left(\mu_1+\xi_1\frac{\theta_1}{2}\right)\sin^2\theta_1 - 2\xi_1\cos\theta_1(\theta_1\cos\theta_1-\sin\theta_1)}{16\left(\mu_1+\xi_1\frac{\theta_1}{2}\right)^2\left(\theta_1^2-\sin^2\theta_1\right) - 4\xi_1^2(\theta_1\cos\theta_1-\sin\theta_1)^2},
\end{aligned} \tag{20}$$

$$\begin{aligned}
\gamma_b &\cong \left(\frac{\kappa_b+1}{\mu_b}\right)\frac{\sin\theta_1(\sin\theta_1+\Delta\theta\cos\theta_1)}{2(\Delta\theta-\sin\Delta\theta)},\\
\delta_b &\cong \left(\frac{\kappa_b+1}{\mu_b}\right)\frac{\cos\theta_1(\cos\theta_1-\Delta\theta\sin\theta_1)}{2(\Delta\theta-\sin\Delta\theta)},\\
\eta_b &\cong \left(\frac{\kappa_b+1}{\mu_b}\right)\frac{(\sin 2\theta_1+\Delta\theta\cos 2\theta_1)}{8(\Delta\theta-\sin\Delta\theta)}
\end{aligned} \tag{21}$$

$$\begin{aligned}
\gamma_2 &= (\kappa_2+1)\left\{\frac{4\left[\mu_2+\xi_2\left(\frac{\theta_2}{2}+\theta_1+\Delta\theta\right)\right][\theta_2-\sin\theta_2\cos(\theta_2+2\theta_1+2\Delta\theta)]}{D_1} - \frac{2\xi_2\sin(\theta_2+2\theta_1+2\Delta\theta)(\theta_2\cos\theta_2-\sin\theta_2)}{D_1}\right\}\\
\delta_2 &= (\kappa_2+1)\left\{\frac{4\left[\mu_2+\xi_2\left(\frac{\theta_2}{2}+\theta_1+\Delta\theta\right)\right][\theta_2+\sin\theta_2\cos(\theta_2+2\theta_1+2\Delta\theta)]}{D_1} + \frac{2\xi_2\sin(\theta_2+2\theta_1+2\Delta\theta)(\theta_2\cos\theta_2-\sin\theta_2)}{D_1}\right\}\\
\eta_2 &= (\kappa_2+1)\frac{4\left[\mu_2+\xi_2\left(\frac{\theta_2}{2}+\theta_1+\Delta\theta\right)\right]\sin\theta_2\sin(\theta_2+2\theta_1+2\Delta\theta)}{D_1} - \frac{2\xi_2\cos(\theta_2+2\theta_1+2\Delta\theta)(\theta_2\cos\theta_2-\sin\theta_2)}{D_1}
\end{aligned} \tag{22}$$

with

$$\begin{aligned}
D_1 = 16&\left[\mu_2+\xi_2\left(\frac{\theta_2}{2}+\theta_1+\Delta\theta\right)\right]^2\\
&\times\left(\theta_2^2-\sin^2\theta_2\right) - 4\xi_2^2(\theta_2\cos\theta_2-\sin\theta_2)^2
\end{aligned}$$

From the boundary conditions along the interfaces $O\Delta_1\,(\theta=\beta_1=\alpha_b=\theta_1)$ and $O\Delta_2(\theta=\beta_b=\alpha_2=\theta_1+\Delta\theta)$ (Figure 2),

$$\begin{aligned}
\bar{u}_r^{(1)}(r,\theta=\beta_1) &= \bar{u}_r^{(b)}(r,\theta=\beta_1),\\
\bar{u}_\theta^{(1)}(r,\theta=\beta_1) &= \bar{u}_\theta^{(b)}(r,\theta=\beta_1),\\
\bar{u}_r^{(b)}(r,\theta=\alpha_2) &= \bar{u}_r^{(2)}(r,\theta=\alpha_2),\\
\bar{u}_\theta^{(b)}(r,\theta=\alpha_2) &= \bar{u}_\theta^{(2)}(r,\theta=\alpha_2),
\end{aligned} \tag{23}$$

the separation of the concentrated force $\mathbf{F}$ in each subwedge,

$$\begin{aligned}
F_{1_x} + F_{b_x} + F_{2_x} &= F_x,\\
F_{1_y} + F_{b_y} + F_{2_y} &= F_y,
\end{aligned} \tag{24}$$

and relations (9), (12) and (20)–(22), it is obtained:

$$\begin{aligned}
&(\eta_1\sin\theta_1-\gamma_1\cos\theta_1)F_{1_x} - (\delta_1\sin\theta_1-\eta_1\cos\theta_1)F_{1_y}\\
&\quad= (\eta_b\sin\theta_1-\gamma_b\cos\theta_1)F_{b_x} - (\delta_b\sin\theta_1-\eta_b\cos\theta_1)F_{b_y},\\
&(\gamma_1\sin\theta_1+\eta_1\cos\theta_1)F_{1_x} - (\eta_1\sin\theta_1+\delta_1\cos\theta_1)F_{1_y}\\
&\quad= (\gamma_b\sin\theta_1+\eta_b\cos\theta_1)F_{b_x} - (\eta_b\sin\theta_1+\delta_b\cos\theta_1)F_{b_y},\\
&[(\eta_b+\gamma_b\Delta\theta)\sin\theta_1 - (\gamma_b-\eta_b\Delta\theta)\cos\theta_1]F_{b_x}\\
&\quad- [(\delta_b+\eta_b\Delta\theta)\sin\theta_1 - (\eta_b-\delta_b\Delta\theta)\cos\theta_1]F_{b_y}
\end{aligned}$$

$$
\begin{aligned}
&= [(\eta_2 + \gamma_2 \Delta\theta)\sin\theta_1 - (\gamma_2 - \eta_2 \Delta\theta)\cos\theta_1] F_{2_x} \\
&\quad - [(\delta_2 + \eta_2 \Delta\theta)\sin\theta_1 - (\eta_2 - \delta_2 \Delta\theta)\cos\theta_1] F_{2_y}, \\
&[(\gamma_b - \eta_b \Delta\theta)\sin\theta_1 + (\eta_b + \gamma_b \Delta\theta)\cos\theta_1] F_{b_x} \\
&\quad - [(\eta_b - \delta_b \Delta\theta)\sin\theta_1 + (\delta_b + \eta_b \Delta\theta)\cos\theta_1] F_{b_y} \\
&= [(\gamma_2 - \eta_2 \Delta\theta)\sin\theta_1 + (\eta_2 + \gamma_2 \Delta\theta)\cos\theta_1] F_{2_x} \\
&\quad - [(\eta_2 - \delta_2 \Delta\theta)\sin\theta_1 + (\delta_2 + \eta_2 \Delta\theta)\cos\theta_1] F_{2_y}, \\
&F_{1_x} + F_{b_x} + F_{2_x} = F_x \\
&F_{1_y} + F_{b_y} + F_{2_y} = F_y
\end{aligned} \tag{25}
$$

After some manipulations, it finally results

$$
\begin{aligned}
&\left(1 + \frac{\eta_1\eta_b - \gamma_1\delta_b}{H_b} + \frac{\eta_1\eta_2 - \gamma_1\delta_2}{H_2}\right) F_{1_x} \\
&\quad + \left(\frac{\eta_1\delta_b - \delta_1\eta_b}{H_b} + \frac{\eta_1\delta_2 - \delta_1\eta_2}{H_2}\right) F_{1_y} = F_x \\
&\left(\frac{\eta_1\gamma_b - \gamma_1\eta_b}{H_b} + \frac{\eta_1\gamma_2 - \gamma_1\eta_2}{H_2}\right) F_{1_x} \\
&\quad + \left(1 + \frac{\eta_1\eta_b - \delta_1\gamma_b}{H_b} + \frac{\eta_1\eta_2 - \delta_1\gamma_2}{H_2}\right) F_{1_y} = F_y \\
&F_{2_x} = \frac{\eta_1\eta_2 - \gamma_1\delta_2}{H_2} F_{1_x} + \frac{\eta_1\delta_2 - \delta_1\eta_2}{H_2} F_{1_y}, \\
&F_{2_y} = \frac{\eta_1\gamma_2 - \gamma_1\eta_2}{H_2} F_{1_x} + \frac{\eta_1\eta_2 - \delta_1\gamma_2}{H_2} F_{1_y} \\
&F_{b_x} = F_x - F_{1_x} - F_{2_x},\ F_{b_y} = F_y - F_{1_y} - F_{2_y},
\end{aligned} \tag{26}
$$

From the solution of system (26), the force components F_{j_x} and F_{j_y} $(j = 1, b, 2)$, are determined.

On the other hand, from relations (6) and (17)$(j = 1, b, 2)$, in the case of an exponentially varying shear modulus, the coefficients γ_j, δ_j and η_j $(j = 1, 2)$, are given by:

$$
\begin{aligned}
\gamma_1 &= \frac{d_1^2(\kappa_1 + 1)}{8\mu_{o_1}} \\
&\quad \times \left\{ \frac{\left(\frac{d_1^2+4}{2d_1} - \sin 2\theta_1 - \frac{d_1}{2}\cos 2\theta_1\right) e^{\frac{1}{2}d_1\theta_1} - \frac{2}{d_1} e^{-\frac{1}{2}d_1\theta_1}}{e^{d_1\theta_1} + e^{-d_1\theta_1} - \left(2 + d_1^2 \sin^2\theta_1\right)} \right\} \\
\delta_1 &= \frac{d_1^2(\kappa_1 + 1)}{8\mu_{o_1}} \\
&\quad \times \left\{ \frac{\left(\frac{d_1^2+4}{2d_1} + \sin 2\theta_1 + \frac{d_1}{2}\cos 2\theta_1\right) e^{\frac{1}{2}d_1\theta_1} - \left(\frac{d_1^2+2}{d_1}\right) e^{-\frac{1}{2}d_1\theta_1}}{e^{d_1\theta_1} + e^{-d_1\theta_1} - \left(2 + d_1^2 \sin^2\theta_1\right)} \right\} \\
\eta_1 &= \frac{d_1^2(\kappa_1 + 1)}{8\mu_{o_1}} \left\{ \frac{\left(\frac{d_1}{2}\sin 2\theta_1 - \cos 2\theta_1\right) e^{\frac{1}{2}d_1\theta_1} + e^{-\frac{1}{2}d_1\theta_1}}{e^{d_1\theta_1} + e^{-d_1\theta_1} - \left(2 + d_1^2 \sin^2\theta_1\right)} \right\}
\end{aligned} \tag{27}
$$

$$
\begin{aligned}
\gamma_2 &= \frac{d_2^2(\kappa_2 + 1)}{8\mu_{o_2}} \\
&\quad \times \left\{ \frac{\left[\frac{d_2^2+4}{2d_2} - \sin 2(\theta_1 + \theta_2 + \theta_b) - \frac{d_2}{2}\cos 2(\theta_1 + \theta_2 + \theta_b)\right] e^{\frac{1}{2}d_2\theta_2}}{D_2} - \frac{\left[\frac{d_2^2+4}{2d_2} - \sin 2(\theta_1 + \theta_b) - \frac{d_2}{2}\cos 2(\theta_1 + \theta_b)\right] e^{-\frac{1}{2}d_2\theta_2}}{D_2} \right\} \\
\delta_2 &= \frac{d_2^2(\kappa_2 + 1)}{8\mu_{o_2}} \\
&\quad \times \left\{ \frac{\left[\frac{d_2^2+4}{2d_2} + \sin 2(\theta_1 + \theta_2 + \theta_b) + \frac{d_2}{2}\cos 2(\theta_1 + \theta_2 + \theta_b)\right] e^{\frac{1}{2}d_2\theta_2}}{D_2} - \frac{\left[\frac{d_2^2+4}{2d_2} + \sin 2(\theta_1 + \theta_b) + \frac{d_2}{2}\cos 2(\theta_1 + \theta_b)\right] e^{-\frac{1}{2}d_2\theta_2}}{D_2} \right\} \\
\eta_2 &= \frac{d_2^2(\kappa_2 + 1)}{8\mu_{o_2}} \left\{ \frac{\left[\frac{d_2}{2}\sin 2(\theta_1 + \theta_2 + \theta_b) - \cos 2(\theta_1 + \theta_2 + \theta_b)\right] e^{\frac{1}{2}d_2\theta_2}}{D_2} - \frac{\left[\frac{d_2}{2}\sin 2(\theta_1 + \theta_b) - \cos 2(\theta_1 + \theta_b)\right] e^{-\frac{1}{2}d_2\theta_2}}{D_2} \right\}
\end{aligned} \tag{28}
$$

with

$$
D_2 = e^{d_2\theta_2} + e^{-d_2\theta_2} - \left(2 + d_2^2 \sin^2\theta_2\right)
$$

with

$$
H_j = \eta_j^2 - \gamma_j\delta_j,\ j = 1, b, 2
$$

For the isotropic infinitesimal sub-region, $j = b\,(\theta_b = \Delta\theta)$, relations (21) because of relations (19), are again valid. The force

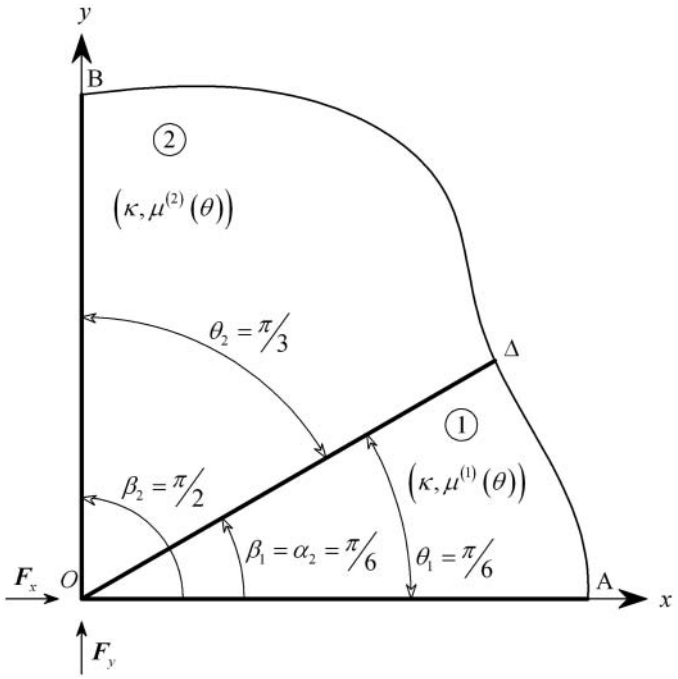

FIG. 3. A graded bi-wedge of angle $\theta = \pi/2$ under a concentrated load at its apex.

components F_{j_x} and F_{j_y} $(j = 1, b, 2)$ are determined from the solution of system (26).

4. APPLICATIONS

Three applications are considered in order to study the influence of the adhesive layer in the elastic behavior of composite wedge. The first one concerns an elastic graded bi-wedge, the second one an elastic composite tri-wedge with a low strength intermediate subwedge whereas the third one an elastic composite tri-wedge with a high strength intermediate subwedge.

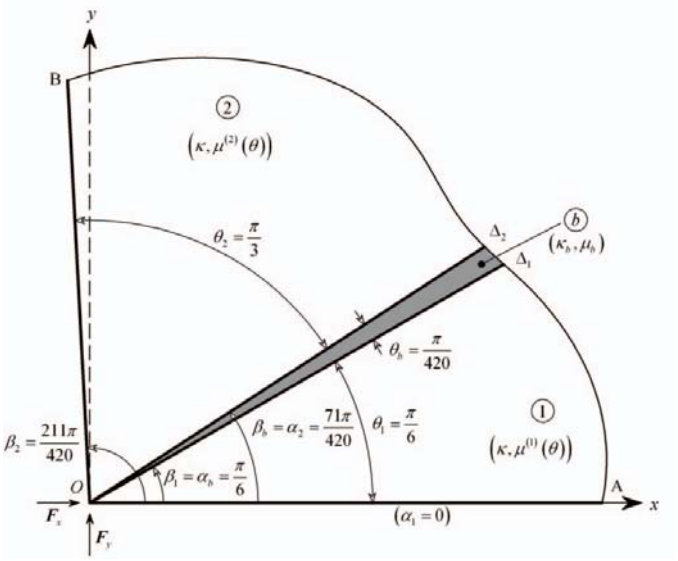

FIG. 4. A composite tri-wedge of angle $\theta \cong \pi/2$ under a concentrated load at its apex.

Let a graded bi-wedge with angles, $\theta_1 = \frac{\pi}{6}$ and $\theta_2 = \frac{\pi}{3}$ $(\theta_w = \theta_1 + \theta_2)$ (Figure 3) in plane strain conditions. In each subwedge a linearly varying shear modulus or an exponentially varying shear modulus, is considered whereas Poisson's ratio is taken constant $(\nu_1 = \nu_2 = \nu, \kappa_1 = \kappa_2 = \kappa)$.

At first, the linearly varying shear modulus in each subwedge, is given by:

$$\begin{aligned}
\mu^{(1)}(\theta) &= \mu_1 + \xi_1\theta = \mu\left(1 - \zeta\frac{\pi}{6}\right) \\
&\quad + 2\zeta\mu\theta,\ \alpha_1\,(=0) \le \theta \le \beta_1\left(=\frac{\pi}{6}\right),\ \theta_1 = \beta_1 - \alpha_1 \\
\mu_1 &= \mu - \xi\frac{\pi}{6},\ \xi_1 = 2\xi,\ \xi = \zeta\mu,\ \mu = \mu^{(1)}\left(\theta = \frac{\alpha_1 + \beta_1}{2}\right), \\
\mu^{(2)}(\theta) &= \mu_2 + \xi_2\theta = \mu\left(2 - \zeta\frac{\pi}{3}\right) \\
&\quad + \zeta\mu\theta,\ \alpha_2\left(=\frac{\pi}{6}\right) \le \theta \le \beta_2\left(=\frac{\pi}{2}\right),\ \theta_2 = \beta_2 - \alpha_2 \\
\mu_2 &= 2\mu - \xi\frac{\pi}{3},\ \xi_2 = \xi,\ \xi = \zeta\mu,\ 2\mu \\
&= \mu^{(2)}\left(\theta = \frac{\alpha_2 + \beta_2}{2}\right),
\end{aligned} \tag{29}$$

where μ, ξ given constants with $\zeta = \xi/\mu = 0.10$. Substituting relations (29) into relations (13), it is finally obtained

$$\begin{aligned}
\gamma_1 &= 0.9625\frac{\kappa+1}{\mu},\ \delta_1 = 9.8853\frac{\kappa+1}{\mu},\ \eta_1 = 2.6315\frac{\kappa+1}{\mu} \\
\gamma_2 &= 0.5366\frac{\kappa+1}{\mu},\ \delta_2 = 0.2189\frac{\kappa+1}{\mu},\ \eta_2 = 0.2690\frac{\kappa+1}{\mu}
\end{aligned} \tag{30}$$

From our analysis the force components in each subwedge are given from relations (16a), and the stress and displacements fields from relations (8), (9), (16b), and (30). The stress and displacements fields are determined in the two particular loading cases ($F_x = 1,\ F_y = 0$) and($F_x = 0,\ F_y = 1$). Every other loading case may arise from the above two cases based on the superposition principle.

- In the case that $F_x = 1,\ F_y = 0$, we have [27]:

$$\begin{aligned}
F_{1_x} &= 0.6893,\ F_{1_y} = 0.1712, \\
F_{2_x} &= 0.3107,\ F_{2_y} = -0.1712
\end{aligned} \tag{31}$$

- In the case that $F_x = 0,\ F_y = 1$ we have:

$$\begin{aligned}
F_{1_x} &= -0.3093,\ F_{1_y} = -0.0671, \\
F_{2_x} &= 0.3093,\ F_{2_y} = 1.0671
\end{aligned} \tag{32}$$

Secondly the exponentially varying shear modulus in each subwedge, is given by:

$$\mu^{(1)}(\theta) = \mu_{o_1} e^{d_1\left(\theta - \frac{\alpha_1+\beta_1}{2}\right)} = \mu e^{d_1(\theta-\pi/12)},$$
$$\alpha_1 (= 0) \le \theta \le \beta_1\left(= \frac{\pi}{6}\right),\ \theta_1 = \beta_1 - \alpha_1,$$
$$\mu_{o_1} = \mu = \mu^{(1)}\left(\theta = \frac{\alpha_1+\beta_1}{2}\right),$$
$$\mu^{(2)}(\theta) = \mu_{o_2} e^{d_2\left(\theta - \frac{\alpha_2+\beta_2}{2}\right)} = 2\mu e^{d_2(\theta-\pi/3)},$$
$$\alpha_2\left(= \frac{\pi}{6}\right) \le \theta \le \beta_2\left(= \frac{\pi}{2}\right),\ \theta_2 = \beta_2 - \alpha_2,$$
$$\mu_{o_2} = 2\mu = \mu^{(2)}\left(\theta = \frac{\alpha_2+\beta_2}{2}\right), \tag{33}$$

where the coefficients d_1 and d_2 are appropriately calculated from relations (4) so that the shear moduli given by relations (33) approximate the shear moduli given by relations (29). This happens in order to obtain almost the same range of variation in the values of shear modules in both, the linearly and the exponentially varying shear modulus, applications. Thus for $\zeta = 0.10$, we have:

$$\zeta_1 = \frac{\xi_1}{\mu_{o_1}} = \frac{2\xi}{\mu} = 2\zeta = 0.20,$$
$$d_1 = -\frac{12}{\pi}\ln\left(1 - 0.20\frac{\pi}{12}\right) = 0.2054,$$
$$\zeta_2 = \frac{\xi_2}{\mu_{o_2}} = \frac{\xi}{2\mu} = \frac{1}{2}\zeta = 0.05,$$
$$d_2 = -\frac{6}{\pi}\ln\left(1 - 0.05\frac{\pi}{6}\right) = 0.0507 \tag{34}$$

Taking into consideration relations (17), (33), and (34), it is obtained

$$\gamma_1 = 0.9624\frac{\kappa+1}{\mu},\ \delta_1 = 9.8765\frac{\kappa+1}{\mu},$$
$$\eta_1 = 2.6304\frac{\kappa+1}{\mu}$$
$$\gamma_2 = 0.5365\frac{\kappa+1}{\mu},\ \delta_2 = 0.2211\frac{\kappa+1}{\mu},$$
$$\eta_2 = 0.2689\frac{\kappa+1}{\mu} \tag{35}$$

For the two particular loading cases ($F_x = 1$, $F_y = 0$) and ($F_x = 0$, $F_y = 1$), the force components in each subwedge are determined from relations (16a), and the stress and displacements fields in each subwedge from relations (8), (9), (16b), and (35).

• In the case that $F_x = 1,\ F_y = 0$, we have:

$$F_{1_x} = 0.6892,\ F_{1_y} = 0.1713,\ F_{2_x} = 0.3108,\ F_{2_y} = -0.1713 \tag{36}$$

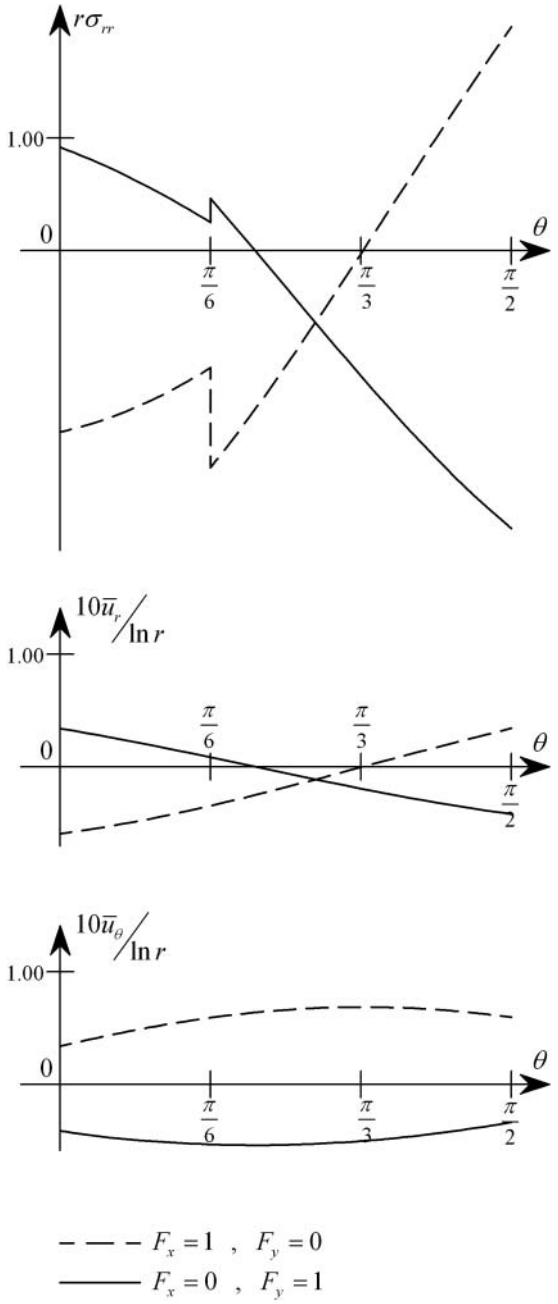

FIG. 5. The dimensionless stress and displacements fields in terms of the angular variation θ of a graded bi-wedge of angle $\theta_w = \pi/2$ in plane strain conditions.

• In case that $F_x = 0$, $F_y = 1$, we have:

$$F_{1_x} = -0.3082,\ F_{1_y} = -0.0666,\ F_{2_x} = 0.3082,\ F_{2_y} = 1.0666 \tag{37}$$

It is observed that the force components with the appropriate determination of the coefficients d_1 and d_2(relation (4) [relations (31), (32)], are almost equal with those calculated in the linear case.

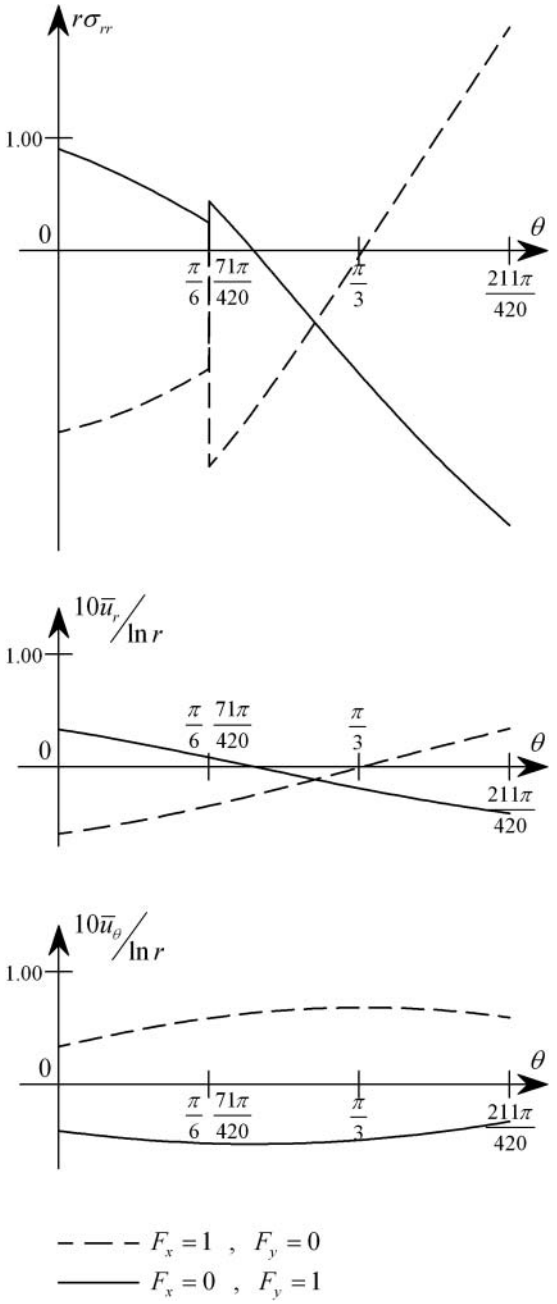

FIG. 6. The dimensionless stress and displacements fields in terms of the angular variation θ of a composite tri-wedge of angle $\theta_w \cong \pi/2$ in plane strain conditions with a low strength intermediate adhesive subwedge.

Let elastic composite tri-wedge (Figure 4) of angles $\theta_1 = \frac{\pi}{6}, \theta_b$ and $\theta_2 = \frac{\pi}{3}$ $(\theta_w = \theta_1 + \theta_b + \theta_2)$ consisting of two graded subwedges $(j = 1, 2)$ and an isotropic intermediate subwedge $(j = b)$, which simulates the infinitesimal adhesive layer (Section 3). In each graded subwedge a linearly varying shear modulus or an exponentially varying shear modulus is considered whereas Poisson's ratio is taken constant($\nu_1 = \nu_2 = \nu$, $\kappa_1 = \kappa_2 = \kappa$). The angle θ_b of the isotropic adhesive subwedge is given by relation (18) for a layer of average thickness, ε, with $1.50mm \le \varepsilon \le 2.00mm$, and a maximum radius of a sector, $R_0 = 500mm$. Thus it is obtained $\theta_b \cong \pi/420rad$.

The linearly varying shear modulus in each graded subwedge and the constant shear modulus in the isotropic subwedge are given by:

$$\mu^{(1)}(\theta) = \mu_1 + \xi_1\theta = \mu\left(1 - \zeta\frac{\pi}{6}\right) + 2\zeta\mu\theta,$$
$$\alpha_1 (= 0) \le \theta \le \beta_1\left(= \frac{\pi}{6}\right), \theta_1 = \beta_1 - \alpha_1,$$
$$\mu_1 = \mu - \xi\frac{\pi}{6}, \quad \xi_1 = 2\xi, \quad \xi = \zeta\mu, \quad \mu = \mu^{(1)}$$
$$\times \left(\theta = \frac{\alpha_1 + \beta_1}{2} = \frac{\pi}{12}\right), \tag{38}$$
$$\mu^{(b)}(\theta) = \mu_b = \text{const.}, \alpha_b \left(= \frac{\pi}{6}\right) \le \theta \le \beta_b$$
$$\times \left(= \frac{71\pi}{420}\right), \quad \theta_b = \beta_b - \alpha_b = \frac{\pi}{420}, \tag{39}$$
$$\mu^{(2)}(\theta) = \mu_2 + \xi_2\theta = \mu\left(2 - \zeta\frac{47\pi}{140}\right)$$
$$+ \zeta\mu\theta, \alpha_2 \left(= \frac{71\pi}{420}\right) \le \theta \le \beta_2$$
$$\times \left(= \frac{211\pi}{420}\right), \quad \theta_2 = \beta_2 - \alpha_2,$$
$$\mu_2 = 2\mu - \xi\frac{47\pi}{140}, \quad \xi_2 = \xi = \zeta\mu, \quad 2\mu = \mu^{(2)}$$
$$\times \left(\theta = \frac{\alpha_2 + \beta_2}{2} = \frac{47\pi}{140}\right), \tag{40}$$

where μ, ξ given constants, with $\zeta = \xi/\mu = 0.10$, $\mu_b = \mu/50$ and $\kappa_b + 1 = 0.85(\kappa + 1)$. From relations (20), (21), and (22), we have:

$$\gamma_1 = 0.9625\frac{\kappa+1}{\mu}, \quad \delta_1 = 9.8853\frac{\kappa+1}{\mu}, \quad \eta_1 = 2.6315\frac{\kappa+1}{\mu}$$
$$\gamma_b = (0.3858 \times 10^8)\frac{\kappa+1}{\mu}, \quad \delta_b = (1.1375 \times 10^8)\frac{\kappa+1}{\mu},$$
$$\eta_b = (0.6624 \times 10^8)\frac{\kappa+1}{\mu}, \quad \gamma_2 = 0.5406\frac{\kappa+1}{\mu},$$
$$\delta_2 = 0.2149\frac{\kappa+1}{\mu}, \quad \eta_2 = 0.2666\frac{\kappa+1}{\mu} \tag{41}$$

- In the case that $F_x = 1$, $F_y = 0$ from relations (8), (9), (12), (26), and (41), it is obtained:

$$F_{1_x} = 0.6911, F_{1_y} = 0.1719, F_{2_x} = 0.3089,$$
$$F_{2_y} = -0.1719, F_{b_x} = 2.2 \times 10^{-5}, F_{b_y} = 1.3 \times 10^{-5}, \tag{42}$$

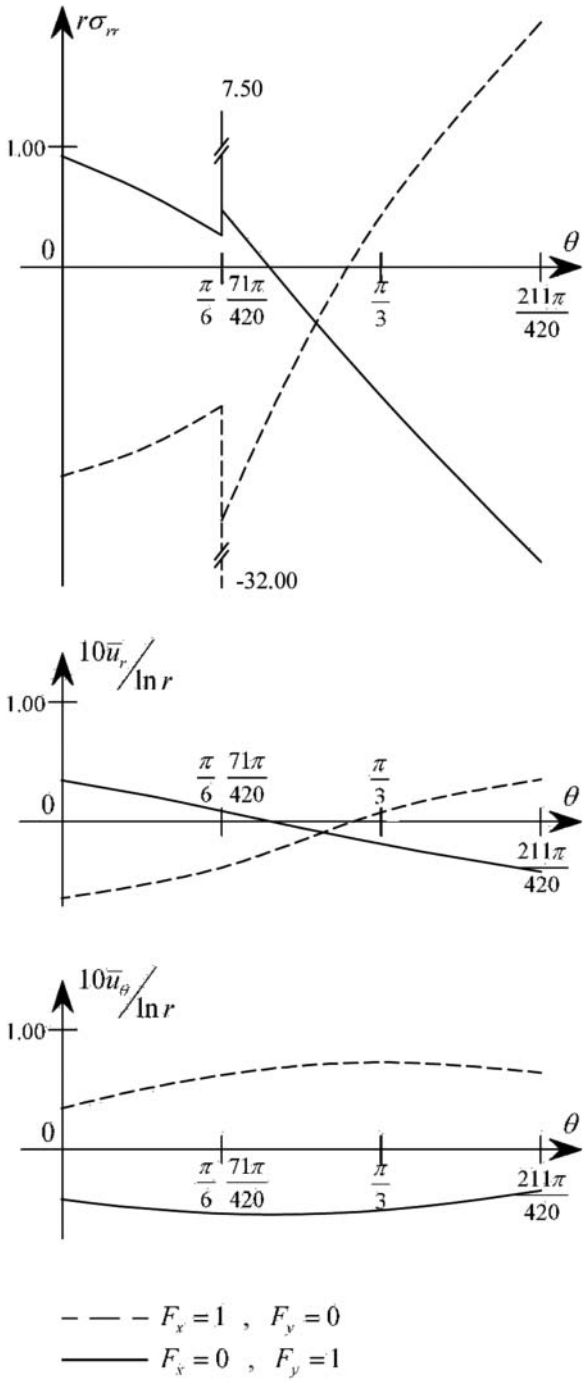

FIG. 7. The dimensionless stress and displacements fields in terms of the angular variation θ of a composite tri-wedge of angle $\theta_w \cong \pi/2$ in plane strain conditions with a high strength intermediate adhesive subwedge.

• In case that $F_x = 0$, $F_y = 1$, we have:

$$F_{1_x} = -0.3052,\ F_{1_y} = -0.0663,\ F_{2_x} = 0.3052,$$
$$F_{2_y} = 1.0663,\ F_{b_x} = -5.1 \times 10^{-6},\ F_{b_y} = -3 \times 10^{-6} \quad (43)$$

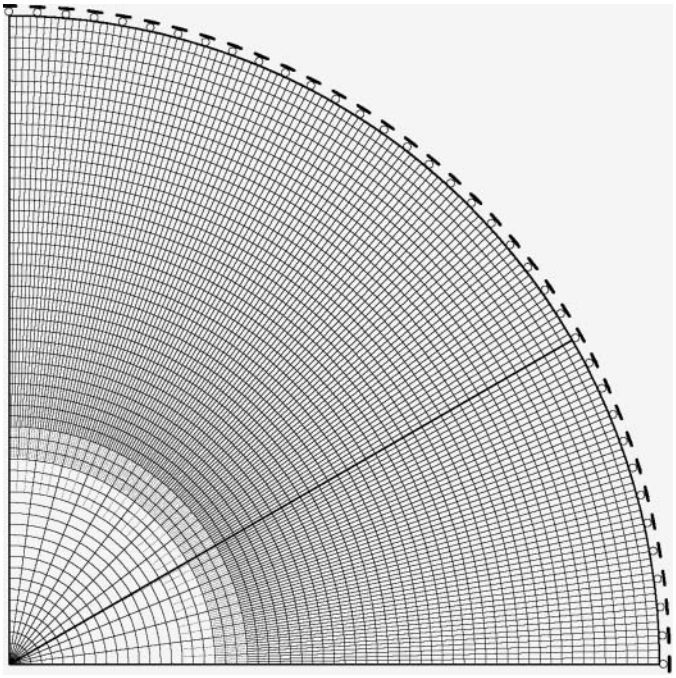

FIG. 8. Finite element mesh for the composite tri-wedge problem.

It is observed that the force components of the adhesive ($j = b$) are very low because of the infinitesimal area of the adhesive wedge taken into consideration.

The exponentially varying shear modulus in each graded subwedge of the tri-wedge (Figure 4), taking into account relations (34), is given by:

$$\mu^{(1)}(\theta) = \mu_{o_1} e^{d_1\left(\theta - \frac{\alpha_1+\beta_1}{2}\right)} = \mu e^{d_1(\theta-\pi/12)},$$
$$\alpha_1\,(=0) \le \theta \le \beta_1\left(=\frac{\pi}{6}\right), \quad \theta_1 = \beta_1 - \alpha_1$$
$$\mu_{o_1} = \mu^{(1)}\left(\theta = \frac{\alpha_1+\beta_1}{2}\right) = \mu, \quad d_1 = 0.2054 \quad (44)$$

$$\mu^{(b)}(\theta) = \mu_b = \text{constant},\ \kappa_b = \text{constant},$$
$$\alpha_b\left(=\frac{\pi}{6}\right) \le \theta \le \beta_b\left(=\frac{71\pi}{420}\right)$$
$$\theta_b = \beta_b - \alpha_b = \frac{\pi}{420} \quad (45)$$

$$\mu^{(2)}(\theta) = \mu_{o_2} e^{d_2\left(\theta - \frac{\alpha_2+\beta_2}{2}\right)} = 2\mu e^{d_2(\theta-47\pi/140)},$$
$$\alpha_2\left(=\frac{71\pi}{420}\right) \le \theta \le \beta_2\left(=\frac{211\pi}{420}\right), \theta_2 = \beta_2 - \alpha_2$$
$$\mu_{o_2} = \mu^{(2)}\left(\theta = \frac{\alpha_2+\beta_2}{2}\right) = 2\mu, d_2 = 0.0507 \quad (46)$$

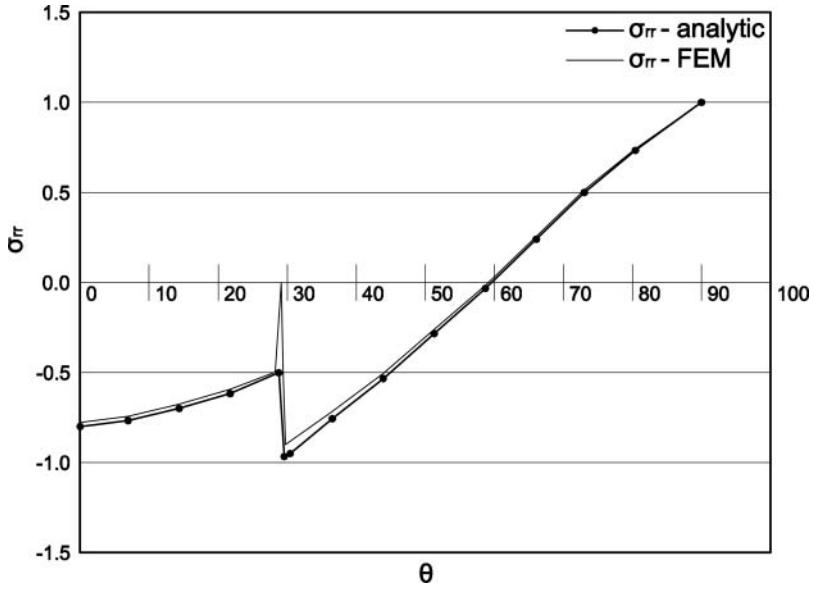

FIG. 9. Comparison of the radial σ_{rr}-stresses in terms of the angular variation θ, in a composite tri-wedge for $r = 200$ mm, between the analytical solution and the Finite Element Analysis for the loading case $F_x = 1$, $F_y = 0$.

Setting $\zeta = 0.10\,(\xi = 0.10\,\mu)$, $\mu_b = \mu/50$, $\kappa_b + 1 = 0.85\,(\kappa + 1)$, from relations (21), (27), and (28), occurs:

$$\gamma_1 = 0.9624\frac{\kappa+1}{\mu},\ \delta_1 = 9.8765\frac{\kappa+1}{\mu},\ \eta_1 = 2.6304\frac{\kappa+1}{\mu},$$
$$\gamma_b = \left(0.3858\times 10^8\right)\frac{\kappa+1}{\mu},\ \delta_b = (1.1375\times 10^8)\frac{\kappa+1}{\mu},$$
$$\eta_b = \left(0.6624\times 10^8\right)\frac{\kappa+1}{\mu},$$
$$\gamma_2 = 0.5405\frac{\kappa+1}{\mu},\ \delta_2 = 0.2148\frac{\kappa+1}{\mu},\ \eta_2 = 0.2665\frac{\kappa+1}{\mu} \tag{47}$$

• In case that $F_x = 1$, $F_y = 0$ from relations (8), (9), (12), (26), and (49), we have:

$$F_{1_x} = 0.6912,\ F_{1_y} = 0.1720,\ F_{2_x} = 0.3088,$$
$$F_{2_y} = -0.1720,\ F_{b_x} = 2.2\times 10^{-5},\ F_{b_y} = 1.3\times 10^{-5}, \tag{48}$$

• In case that $F_x = 0$, $F_y = 1$, we have:

$$F_{1_x} = -0.3051,\ F_{1_y} = -0.0663,\ F_{2_x} = 0.3051,$$
$$F_{2_y} = 1.0663,\ F_{b_x} = -5.1\times 10^{-6},\ F_{b_y} = -3\times 10^{-6} \tag{49}$$

The displacements field in each subwedge of the tri-wedge($j = 1, b, 2$), is given by the same relations (9b) and (10).

The third application concerns an elastic tri-wedge (Figure 4) with elastic properties given by relations (38) and (39), where the shear modulus of each graded subwedge is varying linearly and the infinitesimal adhesive subwedge consists of a high strength material ($\mu_b = 50\mu$). Following the procedure described previously (relations (38)–(43) occurs:

$$F_{1x} = 0.7489F_x - 0.3186F_y,\ \ F_{1y} = 0.1869F_x - 0.0698F_y$$
$$F_{2x} = 0.3631F_x + 0.2913F_y,\ \ F_{2y} = -0.1228F_x + 1.0519F_y$$
$$F_{bx} = -0.1120F_x + 0.0273F_y,\ \ F_{by} = -0.0641F_x + 0.0179F_y \tag{50}$$

The dimensionless stress ($r\sigma_{rr}$) and displacements ($\bar{u}_i/\ln r; i = r, \theta$) fields, in the plane strain case for $\nu = 0.30$ ($\kappa = 3 - 4\nu = 1.80$) and $\mu = 10$ GPa, are plotted for the first application in Figure 5, for the second application in Figure 6, and for the third application in Figure 7. The plots in Figures 5, 6, and 7 are referred only in the case of a linearly varying shear modulus, as the plots resulting for the exponentially varying shear modulus case almost coincide with the above graphics. It is observed that according to our analysis, the influence of the adhesive layer in the stress and displacement fields can be considered as negligible. Hence the adhesive layer may be degenerated into an interface (a subwedge of zero angle) between the two graded subwedges.

The Finite element software ANSYS [28] is used to compute the stress fields in the second application (Figure 4). A two-dimensional finite element model is used for the analysis. The infinite composite tri-wedge is simulated by a finite wedge of a radius $R_0 = 1000$mm(relation (18)). Fixed conditions are applied to the radial direction at $r = R_0$. In the Finite Element Analysis the 8-noded quadrilateral plane strain elements (PLANE 82) are used [28]. The area of the wedge apex is modeled with the 6-noded triangular plane strain elements (PLANE 2). 11000 elements with almost 33300 nodes constitute

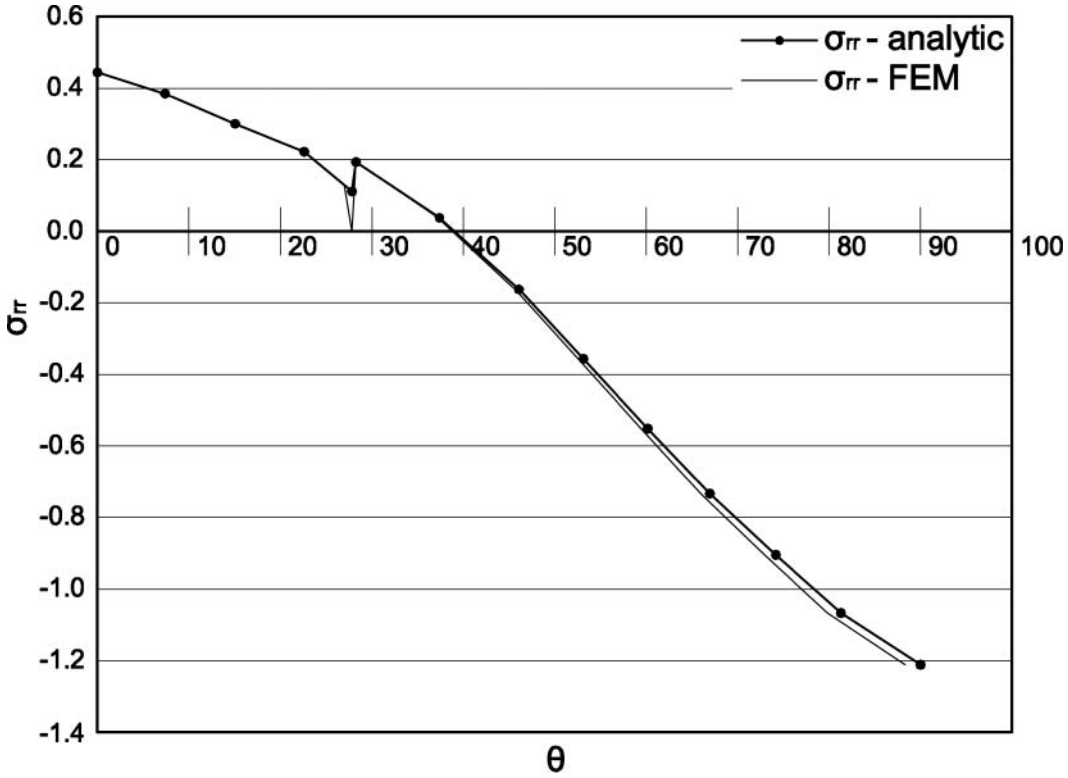

FIG. 10. Comparison of the radial σ_{rr}-stresses in terms of the angular variation θ, in a composite tri-wedge for $r = 200$ mm, between the analytical solution and the finite element analysis for the loading case $F_x = 0$, $F_y = 1$.

the Finite Element Mesh (FEM) (Figure 8). In the Finite Element Mesh the angularly varying shear modulus is simulated by an angularly step varied modulus in every 7,5° degrees. The FEM is uniform in the radial direction with 60 equal length elements.

The radial stress fields calculated analytically and numerically using the Finite Element Analysis, for the loading cases ($F_x = 1$, $F_y = 0$) and ($F_x = 0$, $F_y = 1$), are plotted at the arc $r = 200$mm in Figures 9 and 10, respectively. It is observed that the agreement between the proposed analytical solution and the numerical solution is good and the percentage differences are insignificant.

5. CONCLUSIONS

In our study an analytical approach was developed in order to determine the stress and displacement fields not close to the singular point at the apex of a graded bi-wedge, loaded by a concentrated force at its apex. The proposed study is based on the self-similarity property, on the separation of loading in each subwedge and on the continuity of stress and displacements fields at the interfaces between the subwedges.

In this paper an analytical approach was also developed for the influence of a wedge-adhesive layer in an elastic graded bi-wedge loaded by a concentrated force at its apex. The adhesive layer in the bi-wedge was considered either by an interface (a layer of zero thickness) between the two graded subwedges or by an intermediate infinitesimal subwedge of very small wedge-angle, with elastic constants those of an isotropic adhesive material. Hence, with the proposed procedure, a tri-material junction consisting of two graded subwedges bonded to an infinitesimal adhesive subwedge was investigated.

The graded character of the subwedges was studied either by a linearly varying or an exponentially varying shear modulus. The linearly varying shear modulus may be successfully substituted by an exponentially varying shear modulus based on the appropriately selected exponential coefficients.

By means of the first and the second applications (Section 4) it was found that independently from the consideration of a low strength adhesive subwedge($\mu_b = \mu/50$), the stress and displacement fields of the subwedges almost coincide (Figures 5 and 6). In the case that an infinitesimal subwedge simulates the adhesive layer, its radial stress field was practically negligible. Thus, the composite tri-material junction can be, with a great accuracy, reduced to a two-material junction, eliminating the adhesive infinitesimal subwedge. The stress fields that appeared in Figures 5 and 6 show that in absolute values, the radial σ_{rr}-stresses are sufficiently higher in the radius for $\theta = \pi/2$ than in the radius for $\theta = 0$. This is due to the considered variation of the shear moduli in the graded subwedges. However, in the case of a high strength adhesive subwedge$(\mu_b = 50\mu)$, an increase of the stress field of the graded subwedges (Figure 6) at the neighborhood of the adhesive subwedge, up to 10% was observed.

When the shear modulus of the adhesive layer increases, then as expected, the radial stresses of the adhesive increase, too. This increase causes a radial stress concentration of the graded subwedges at the neighborhood of the adhesive. On the other hand the plots of the stress and displacement fields (Figure 7) remain similar to those of Figures 5 and 6. The stress fields in the case of the low strength adhesive subwedge were also calculated by the Finite Element Analysis. A comparison was made with the proposed analytical solution and a good agreement was achieved (Figures 9 and 10).

In our study we try to confront the influence of an isotropic adhesive layer between two graded subwedges. In the case that the adhesive layer is simulated either by an interface or by an infinitesimal isotropic subwedge, the problem remains self-similar in linear elasticity, and no shear and normal interactions ($\sigma_{r\theta} = \sigma_{\theta\theta} = 0$) appear in any radial line of the composite wedge. In the case that the adhesive layer is simulated by a layer of constant thickness, the geometrical symmetry is not valid any more, and thus the problem does not remain self-similar and the stress field does not remain radial. This means that shear and normal interactions appear at the interfaces among the graded subwedges and the adhesive layer ($\sigma_{r\theta} \neq 0$, $\sigma_{\theta\theta} \neq 0$). The adhesive layer of constant thickness between the two subwedges may be treated only numerically via the Finite element method. In the case of a constant thickness adhesive layer, it is expected that the stress field, due to the interactions among the subwedges and the adhesive layer, is mainly in shear.

REFERENCES

1. S.G. Lekhnitskii, Theory of Elasticity of an Anisotropic Elastic Body, Holden-Day, San Francisco, 1963.
2. S.c. Cowin, Torsion of Cylinders with Intrinsic Orthotropy. ASME, J. Appl. Mechanics., vol, 109, pp. 778–782, 1987.
3. F. Delale, and F. Endogan, On the Mechanical Modeling of the Interfacial Region in Bonded Half-Planes. ASME, Journal of Applied Mechanics., vol, 55, pp. 317–324, 1988.
4. F. Erdogan, A.C. Kaya, and P.F. Joseph, The Crack Problem in Bonded Nonhomogeneous Materials. ASME, Journal of Applied Mechanics., vol. 58, pp. 410–418, 1991.
5. J.R. Barber, Elasticity, First Edition, Kluwer Academic Publishers, The Netherlands, 1992.
6. G.A. Maugin, Material Inhomogeneities in Elasticity, Chapman & Hall, London, 1993.
7. S. Nemat-Nasser, and M. Hori, Micromechanics, Overrall Properties of Heterogeneous Materials, North-Holland, Amsterdam, 1993.
8. M.Y. Chung, and T.C. T. Ting, Line Forces and Dislocations In Angularly Inhomogeneous Anisotropic Piezoelectric Wedges and Spaces. Philos.Magazine A., vol. 71, pp. 1335–1343, 1995.
9. J. Aboudi, M.-Z. Pindera, and S.M. Arnold, Thermo-Inelastic Response of Functionally Graded Materials. I. Journal of Solids and Structures., vol. 32, pp. 1675–1710, 1995.
10. T.C. T. Ting, Anisotropic Elasticity—Theory and Applications, Oxford University Press, New York, Oxford, 1996.
11. P.F. Joseph, and N. Zhang, Multiple Root Solutions, Wedge Paradoxes and Singular Stress States That are not Variable—Separable. Compos. Sci. Technol., vol. 58, pp. 1839–1859, 1998.
12. Y.Y. Lin and J.C. Sung, Stress Singularities at the Apex of a Dissimilar Anisotropic Wedge. J.Appl., Mech., vol. 65, pp. 454–463, 1998.
13. J. Aboudi, M.J. Pindera and S.M. Arnold, Higher-Order Theory for Functionally Graded Materials. Composites Part B: Eng. vol. 30B, pp. 777–832, 1999.
14. V.I.Alshits, and O.K. Kirchner, Cylindrically Anisotropic, Radially Inhomogeneous Elastic Materials. Proc. R. Society London A., vol. 457, pp. 671–693, 2001.
15. P. Poonsawat, A.C. Wijeyewickrema and P. Karasudhi, Singular Stress Fields of Angle—Ply and Monoclinic Bimaterial Wedge. Internat. J. Solids Struct., vol. 38, pp. 91–113, 2001.
16. G.H. Paulino, Z. -H. Jin, and R.H. Dodds, Jr, Failure of Functionally Graded Materials In:Karihaloo, B. et al. (Eds.), Encyclopedia of Comprehensive Structural Integrity, Vol. 2, Elsevier, Amsterdam, pp. 607–642, 2003.
17. W.L. Yin, Anisotropic Elasticity and Multi—Material Singularities, Journal of Elasticity., vol. 71, pp. 263–292, 2003.
18. A. Barroso, V. Mantič and F. Paris, Singularity Analysis of Anisotropic Multimaterial Corners, I. Journal of Fracture., vol. 119, pp. 1–23, 2003.
19. E.E. Theotokoglou, and I.H. Stampouloglou, The Sandwich Wedge Under a Concentrated Load at the Apex, Proceedings of the 6th International Conference on Sandwich Structures, Ft. Lauderdale, Florida, Editors J.R. Vinson, Y.D. S. Rajapakse and L.A. Carlsson, pp. 657–671, March 31-April 2, 2003.
20. E.E. Theotokoglou, and I.H. Stampouloglou, The Plane Wedge Problem Loaded at its Apex, the Self—Similarity Property and the Characteristic Vector. Journal of Elasticity., vol. 76, pp. 21–43, 2004.
21. I.H. Stampouloglou, and E.E. Theotokoglou, The anisotropic and Angularly Inhomogeneous Elastic Wedge Under A Monomial Load Distribution, Archive of Applied Mech., vol. 75, pp. 1–17, 2005.
22. A. Carpinteri, and M. Paggi, On the Asymptotic Stress Field in Angularly Nonhomogeneous Materials, Int. Journal of Fracture Mech., vol. 135, pp. 267–283, 2005.
23. G.H. Paulino, H.M. Yin, and L.Z. Sun, Micromechanics-Based Interfacial Debonding Model for Damage of Functionally Graded Materials with Partial Interactions, Int. Journal of Damage Mech. vol. 15, pp. 267–288, 2006.
24. I.H. Stampouloglou, Problems of Elastostatic Wedges. Ph.D. Thesis, National Technical University of Athens 2006.
25. A.P.S. Selvadurai, The Analytical Method In Geomechanics, Applied Mechanics Reviews, vol. 60, pp. 87–106, 2007.
26. R.D. Adams, and W.C. Wake, Structural Adhesive Joints in Engineering, Elsevier Applied Sciences Publishers, 1984.
27. S. Wolfram, Mathematica, A System for Doing Mathematics by Computer. Addison—Wesley, Redwood City, 1991.
28. ANSYS Engineering Analysis system. User's Manuals, Swanson Analysis Systems Inc., 1992.